THE JOURNAL OF BIOLOGICAL CHEMISTRY VOL. 285, NO. 11, pp. 8481–8491, March 12, 2010

The p40/ARPC1 Subunit of Arp2/3 Complex Performs Multiple Essential Roles in WASp-regulated Actin Nucleation*[S]

Received for publication, August 11, 2009, and in revised form, January 11, 2010 Published, JBC Papers in Press, January 12, 2010, DOI 10.1074/jbc.M109.054957

Heath I. Balcer, Karen Daugherty-Clarke, and Bruce L. Goode[1]

From the Department of Biology, Brandeis University, Waltham, Massachusetts 02454

The Arp2/3 complex is a conserved seven-subunit actin-nucleating machine activated by WASp (Wiskott Aldrich syndrome protein). Despite its central importance in a broad range of cellular processes, many critical aspects of the mechanism of the Arp2/3 complex have yet to be resolved. In particular, some of the individual subunits in the complex have not been assigned clear functional roles, including p40/ARPC1. Here, we dissected the structure and function of *Saccharomyces cerevisiae* p40/ARPC1, which is encoded by the essential *ARC40* gene, by analyzing 39 integrated alleles that target its conserved surfaces. We identified three distinct sites on p40/ARPC1 required for function *in vivo*: one site contacts p19/ARPC4, one contacts p15/ARPC5, and one site resides in an extended structural "arm" of p40/ARPC1. Using a novel strategy, we purified the corresponding lethal mutant Arp2/3 complexes from yeast and compared their actin nucleation activities. Lethal mutations at the contact with p19/ARPC4 specifically impaired WASp-induced nucleation. In contrast, lethal mutations at the contact with p15/ARPC5 led to unregulated ("leaky") nucleation in the absence of WASp. Lethal mutations in the extended arm drastically reduced nucleation, and the same mutations disrupted the ability of the purified p40/ARPC1 arm domain to bind the VCA domain of WASp. Together, these data indicate that p40/ARPC1 performs at least three distinct, essential functions in regulating Arp2/3 complex-mediated actin assembly: 1) suppression of spontaneous nucleation by the Arp2/3 complex, which requires proper contacts with p15/ARPC5; 2) propagation of WASp activation signals via contacts with p19/ARPC2; and 3) direct facilitation of actin nucleation through interactions of the extended arm with the VCA domain of WASp.

Regulated assembly of actin networks by the Arp2/3 complex is essential for cell motility, intracellular transport, remodeling of cell shape, and endocytosis. The Arp2/3 complex binds to the sides of pre-existing (mother) actin filaments and nucleates the formation of new (daughter) filaments at a 70-degree angle, leading to the assembly of branched, "arborized" arrays (1, 2). Efficient nucleation by the Arp2/3 complex requires conformational rearrangements of its subunits and its actin monomer recruitment, both of which are triggered by interactions with a nucleation promoting factor (NPF)[2] such as WASp (Wiskott Aldrich syndrome protein; reviewed in Ref. 2). Despite the central importance of WASp-Arp2/3 complex activity in facilitating a wide range of actin-based processes *in vivo*, our understanding of the activation and nucleation mechanism has remained limited.

The Arp2/3 complex is comprised of two actin-like subunits (Arp2 and Arp3), one 40-kDa WD repeat-containing subunit that folds into a β-propeller (p40/ARPC1), and four structurally unique subunits (p35/ARPC2, p21/ARPC3, p19/ARPC4, and p15/ARPC5) (3). Arp2 and Arp3 have been hypothesized to form a pseudo-actin dimer that seeds polymerization of the daughter filament (4). However, the crystal structure of inactive bovine Arp2/3 complex showed that Arp2 and Arp3 are well separated before activation (3). This led to the hypothesis that WASp binding induces conformational changes that drive Arp2 and Arp3 closer together to mimic the barbed end of a filament, which has been supported by fluorescence resonance energy transfer and coupled electron microscopy and single particle analyses (3, 5, 6). More recent evidence suggests further that WASp binding may induce conformational rearrangements that propagate through all seven subunits of the Arp2/3 complex (5, 6). The p35/ARPC2 and p19/ARPC4 subunits form the structural core of the complex and mediate binding to the side of the mother filament (3, 7–10). Functions of the remaining three subunits have remained elusive. p21/ARPC3 has been implicated in NPF binding (11), but it is the only subunit in *Saccharomyces cerevisiae* that can be deleted without causing severe cell growth defects (12). Chemical cross-linking experiments suggest that NPFs interact with three additional subunits (Arp2, Arp3, and p40/ARPC1) (13, 14). Relatively little is known about the functional roles of the p40/ARPC1 and p15/ARPC5 subunits. Both are essential for cell viability in *S. cerevisiae* (12), but the nature of their functional contributions to actin assembly has remained unclear.

Two biochemical studies found that the Arp2/3 complex lacking p40/ARPC1 shows severely reduced actin nucleation activity *in vitro* (8, 15). p40/ARPC1 also binds to the VCA (verprolin homology domain, connector, acidic) domain of *S. cerevisiae* WASp (Las17) (15, 16) and directly contacts two other subunits in the complex, p19/ARPC4 and p15/ARPC5 (3). In

* This work was supported, in whole or in part, by National Institutes of Health Grants GM63691 and GM083137 (to B. G.). This work was also supported by March of Dimes Grant MOD 1-FY07-508.

[S] The on-line version of this article (available at http://www.jbc.org) contains supplemental Figs. S1–S3.

[1] To whom correspondence should be addressed: Dept. of Biology, Rosenstiel Basic Medical Sciences Research Center, Brandeis University, 415 South St., Waltham, MA 02454. Tel.: 781-736-2464; Fax: 781-736-2405; E-mail: goode@brandeis.edu.

[2] The abbreviations used are: NPF, nucleation promoting factor; GST, glutathione *S*-transferase; HA, hemagglutinin; RMA, rabbit skeletal muscle actin.

addition, p40/ARPC1 has been implicated in binding to the mother filament (17) and stabilizing the mother-daughter branch to prevent rocking (9, 18). However, the precise mechanistic contributions of p40/ARPC1 to actin nucleation have been difficult to resolve further without having specific alleles that uncouple its physical interactions and functions.

Here, we dissected p40/ARPC1 structure and function in *S. cerevisiae* by generating a large collection of integrated charge-to-alanine alleles. Our analysis shows that intersubunit contacts of p40/ARPC1 with p19/ARPC4 and p15/ARPC5 are essential for activating and repressing Arp2/3 complex-mediated actin nucleation, respectively. Further, we show that the p40/ARPC1 extended arm domain binds to that WASp VCA domain and that mutations disrupting this interaction severely impair actin nucleation and are lethal *in vivo*. Together, these data identify three distinct conserved surfaces on p40/ARPC1 that are essential *in vivo* and reveal that p40/ARPC1 performs multiple roles in regulating actin nucleation.

EXPERIMENTAL PROCEDURES

Strains, Media, and Plasmid Construction—Standard methods were used for growth and transformation of yeast (19). The *ARC40* open reading frame plus 300 bp upstream and 300 bp downstream genomic DNA sequence was PCR-amplified and ligated into the BamHI and NotI sites of pBluescript II, yielding pBG636. A BglII site was introduced 203 bp upstream of the *ARC40* start codon in pBG636 by QuikChange site-directed mutagenesis (Stratagene; La Jolla, CA), yielding pBG637. The *LEU2* open reading frame plus 903 bp upstream and 850 bp downstream sequence was excised from pBG102 (20) by digestion with BglII and ligated into the BglII site of pBG637, generating pBG638. All of the *arc40* mutations were generated in pBG638 by site-directed mutagenesis, with each allele containing a unique and silent restriction site. All of the plasmids were DNA-sequenced.

The alleles were integrated at the *LEU2* locus of either the diploid strain BGY84 (MATa/α *ade2-101/ADE2 his3Δ200/his3Δ200 leu2–3,112/leu2-3,112 lys2-801/LYS2 ura3-52/ura3-52 arc40Δ::HIS3/ARC40*) or the haploid strain BGY89 (MATa *arc40Δ::HIS3 ade2-101 his3Δ200 leu2-3,112 lys2-801 ura3–52,* pRS316-*ARC40-URA3*). Wild type and mutated pBG638 plasmids were linearized with NsiI and transformed into yeast, and clones were selected on Leu^- medium. Diploid integration strains were sporulated, tetrads were dissected, and Leu^+ His^+ colonies were selected. Integration of each allele was confirmed by PCR-amplifying the *ARC40* locus from genomic DNA and verifying the specific digestion patterns. Haploid strains carrying the integrated alleles were generated and verified similarly after selection on Leu^- medium and tested for lethality by plating on medium containing 5-fluoroorotic acid. Strains with integrated *arc40* alleles generated by the two methods yielded indistinguishable phenotypes (not shown). To generate the plasmid for purifying the Arc40 extended arm domain from *Escherichia coli*, a PCR product encoding Arc40 residues 306–355 was amplified from pBG638 and ligated into the BamHI and NotI sites of pET-GST-TEV (21), producing pBG302.

To generate a yeast strain for the isolation of Arp2/3 complexes containing lethal *arc40* alleles, we integrated different epitope tags at the C termini of two different subunits of the Arp2/3 complex. We first integrated a TEV-3×HA tag at the C terminus of *ARC18* using a modified version of the plasmid pML9 (22), pML9-T, which includes a TEV protease recognition sequence (6). The PCR product was integrated by homologous recombination into the haploid strain BGY12 (MATα *ade2-1 his3-11,15 leu2-3,112 psi$^+$ ssd$^-$ trp1-1 ura3-52*). Integration was confirmed by PCR analysis and immunoblotting whole cell extracts with anti-HA antibodies. Second, we integrated a 3×HA tag at the C terminus of the wild type copy of *ARC40* using pML9 into the haploid strain BGY10 (MATa *ade2-1 his3–11,15 leu2-3,112 psi$^+$ ssd$^-$ trp1-1 ura3-52*), which is isogenic to BGY12. The integration was verified as above. The two haploid strains carrying the distinct tags were mated, diploids were sporulated, and tetrads were dissected. Haploids carrying both tags (on *ARC18* and *ARC40*) were verified by immunoblotting. The resulting double-tagged haploid strain (BGY960) was used to integrate wild type and mutant *ARC40* alleles at the *LEU2* locus using integration plasmids as described above.

Purification of Arc40 Extended Arm—To express the GST-Arc40-arm in *E. coli*, pBG302 was transformed into BL21 (DE3) cells. One liter of cells was grown at 37 °C to an A_{600} level of ~0.5 in LB medium containing 100 μg/ml kanamycin and then induced for 3 h with addition of 0.4 mM isopropyl β-D-thiogalactopyranoside. The cells were pelleted, resuspended in 10 ml of phosphate-buffered saline (20 mM sodium phosphate buffer, 150 mM NaCl, pH 7.4), and frozen at −80 °C. The pellet was thawed in the presence of protease inhibitors (0.5 μg/ml each of antipain, leupeptin, pepstatin A, chymostatin, and aprotinin) and 1 mM phenylmethylsulfonyl fluoride, and then the cells were lysed by sonication. The lysates were centrifuged at 21,000 × *g* for 15 min, and the resulting supernatant was incubated for 1 h at 4 °C with 1 ml of glutathione-agarose beads (Sigma-Aldrich). The beads were washed three times with 15 ml of HEK (20 mM Hepes, 1 mM EDTA, 50 mM KCl, pH 7.5), twice with 15 ml of HEK_{500} (20 mM Hepes, 1 mM EDTA, 500 mM KCl, pH 7.5), twice with 15 ml of HEK, and three times with 15 ml of 150 mM Tris, pH 8.3. The GST-Arc40-arm was either 1) eluted as a GST fusion from beads for 30 min at 4 °C with 30 mM glutathione, 150 mM Tris, pH 8.3, or 2) released from GST by digestion for 2 h at room temperature with 20 units TEV protease (Invitrogen). Glutathione-eluted GST-Arc40-arm was exchanged into HEK buffer, aliquoted, and frozen in liquid N_2. TEV-released Arc40-arm was purified further on a monoQ column (GE Healthcare) and fractionated to the flow-through. The protein was concentrated to 200 μl, aliquoted, and frozen in liquid N_2.

Purification of Mutant and Wild Type Arp2/3 Complexes—Wild type and mutant Arp2/3 complexes were isolated from variants of the yeast strain BGY960 carrying different *arc40* alleles integrated at the *LEU2* locus (strains described above). Yeast cells were grown to an A_{600} level of ~1.0 in YPD medium, pelleted, washed, frozen in liquid N_2, and lysed as described (23). 5–10 grams of frozen cells were thawed in the presence of protease inhibitors and 1 mM phenylmethylsulfonyl fluoride

and then centrifuged at 265,000 × *g* for 20 min at 4 °C. The clarified extract was incubated for 1 h at 4 °C with 50 μl of CL-4B beads (GE Healthcare) coated with HA antibodies (HA.11; Covance, Princeton, NJ). The beads were washed three times with 1.5 ml of HEK, once with 1.5 ml of HEK_{500}, and twice more with 1.5 ml of HEK and then resuspended to generate a 100-μl slurry (50 μl of beads in 50 μl of HEK buffer). The Arp2/3 complex was released from beads by digestion with 20 units of TEV protease (Invitrogen) for 2 h at room temperature. Released Arp2/3 complex was harvested and incubated for 30 min at 4 °C with HA antibody-coated beads to remove any contaminating Arp2/3 complex containing endogenous wild type Arc40-HA. Endogenous Arc40 depletion was assessed by immunoblotting samples from each stage of the purification with anti-HA antibodies (not shown), which verified that preparations contained less than 2% endogenous Arp2/3 complex. The proteins were aliquoted, frozen in liquid N_2, and stored at −80 °C. This preparation typically yields 100 μl of 0.1–0.3 μM Arp2/3 complex, similar to what has been previously described for lethal *arc35* Arp2/3 complexes (10). Based on Western blotting, 60–80% of the total Arp2/3 complex in the cells is isolated in the initial purification step, and 25–50% of this total material is the untagged mutant (or control wild type) Arp2/3 complex, which is isolated in the subsequent step of the preparation.

Additional Protein Purification—Rabbit skeletal muscle actin (RMA) was purified as described (24) and gel-filtered. Pyrenyliodoacetamide-labeled RMA was prepared as described (25, 26). Full-length Las17/WASp and the VCA domain were purified as described (27). Yeast actin was purified as described (23).

Antibodies—Anti-HA (HA.11) mouse monoclonal antibody and anti-GST rabbit antibody were purchased from Covance. Anti-HA horseradish peroxidase-conjugated antibody and anti-Arp2 goat antibody were purchased from Santa Cruz Biotechnology (Santa Cruz, CA). Anti-Las17-VCA domain polyclonal antibody was raised in chickens (Aves labs, Tigard, OR). For immunoblotting, the following antibody dilutions were used: anti-GST (1:1,000), anti-HA horseradish peroxidase (1:1,000), anti-VCA (1:1,000), and anti-Arp2 (1:100).

Actin Assembly Kinetics—Actin assembly kinetics were measured using the pyrene-actin fluorescence assay. The reactions (60 μl) contained 2 μM RMA unless otherwise indicated. 47 μl of gel-filtered monomeric RMA (10% pyrene-labeled) in G buffer (5 mM Tris, pH 7.5, 0.2 mM $CaCl_2$, 0.2 mM dithiothreitol, 0.2 mM ATP) was mixed with 10 μl of HEK buffer or proteins in HEK buffer and then mixed immediately with 3 μl of 20× initiation buffer (1 M KCl, 40 mM $MgCl_2$, 10 mM ATP). Fluorescence was monitored by excitation at 365 nm and emission at 407 nm in a fluorescence spectrophotometer (Photon Technology International, Birmingham, NJ) held at 25 °C. In supplemental Fig. S3, the activities of wild type and *arc40-140* Arp2/3 complex, in the presence and absence of Las17, were compared using RMA *versus* yeast actin.

Las17/WASp Binding Assays—In one set of binding assays (see Fig. 5*A*), control beads or beads coated with full-length Las17/WASp or its VCA domain were incubated for 10 min with 2 μM soluble Arc40-arm in HEK buffer. The beads were pelleted, and the percentage of Arc40-arm bound was determined by analyzing pellet and supernatant fractions on Coomassie-stained gels. In the second set of binding assays (see Fig. 5*B*), control beads or beads coated with wild type GST-Arc40-arm or mutant GST-Arc40–140-arm were incubated with 100 nM Las17/WASp plus 1 mg/ml bovine serum albumin in HEK buffer. The beads were pelleted, and the amount of Las17/WASp bound was determined by immunoblotting supernatant fractions with anti-VCA antibodies and densitometry. In the third set of assays (see Fig. 5*C*), beads coated with the GST-VCA domain were incubated for 10 min with 75 nM wild type *ARC40*, *arc40Δ311–340*, or *arc40-140* Arp2/3 complex in HEK buffer. The beads were pelleted, and the amount of Arp2 bound was determined by immunoblotting pellet fractions with anti-Arp2 antibodies and densitometry.

RESULTS

Charge to Alanine Scan Mutagenesis—To dissect the role of the p40/ARPC1 subunit of Arp2/3 complex, we integrated a large collection of charge-to-alanine substitution alleles, replacing the wild type *S. cerevisiae* gene (*ARC40*) and analyzing mutant effects in haploid strains. Similar mutagenesis strategies have been used to dissect the structure and function of other key actin regulators, including cofilin, profilin, and Cdc42 (28–30). When this work was initiated, the crystal structure of p40/ARPC1 had not yet been reported. For this reason, we could not initially take a structurally guided mutagenesis approach (see below). Using an alignment of p40/ARPC1 sequences from distantly related species, we targeted for site-directed mutagenesis all clusters of two or more conserved charged residues (Arg, Asp, Glu, and Lys) within a window of five residues (Fig. 1), because charged clusters tend to reside on the surface of a protein.

A total of 30 unique *arc40* alleles were initially constructed (Table 1, *arc40-101* to *arc40-133*). Each allele was chromosomally integrated into a wild type diploid yeast strain (BGY84), and diploids were sporulated and tetrads were dissected to obtain haploids. After the crystal structure of bovine p40/ARPC1 was reported (3) (Fig. 2*A*), it became evident that the mutations we generated are distributed among all seven blades of the β-propeller structure (Figs. 1 and 2*B*). To our surprise, not a single allele in this initial collection (*arc40-101* through *arc40-133*) caused strong defects in cell growth (Fig. 2*C*) or actin organization (not shown). Only one allele, *arc40-118*, caused any phenotype. This mutant showed no obvious defects in cell morphology or actin organization at the nonpermissive temperature but exhibited partially impaired growth at an elevated temperature (37 °C) (supplemental Fig. S1).

Revised Strategy to Define Essential Surfaces—The lack of overt growth phenotypes in such an extensive allele collection of an essential gene was unexpected and a bit puzzling. One possibility we considered was that no single allele had been effective in disrupting important p40/ARPC1 interactions. To address this idea, we modeled the positions of our alleles on the structure of bovine p40/ARPC1 (Fig. 2, *A* and *B*). This revealed that a number of our *arc40* alleles that were well separated in the primary sequence were actually adjacent on the surface of the p40/ARPC1 structure (Figs. 1 and 2*B*). Using this information to guide us, we next tested the effects of combined pairs of

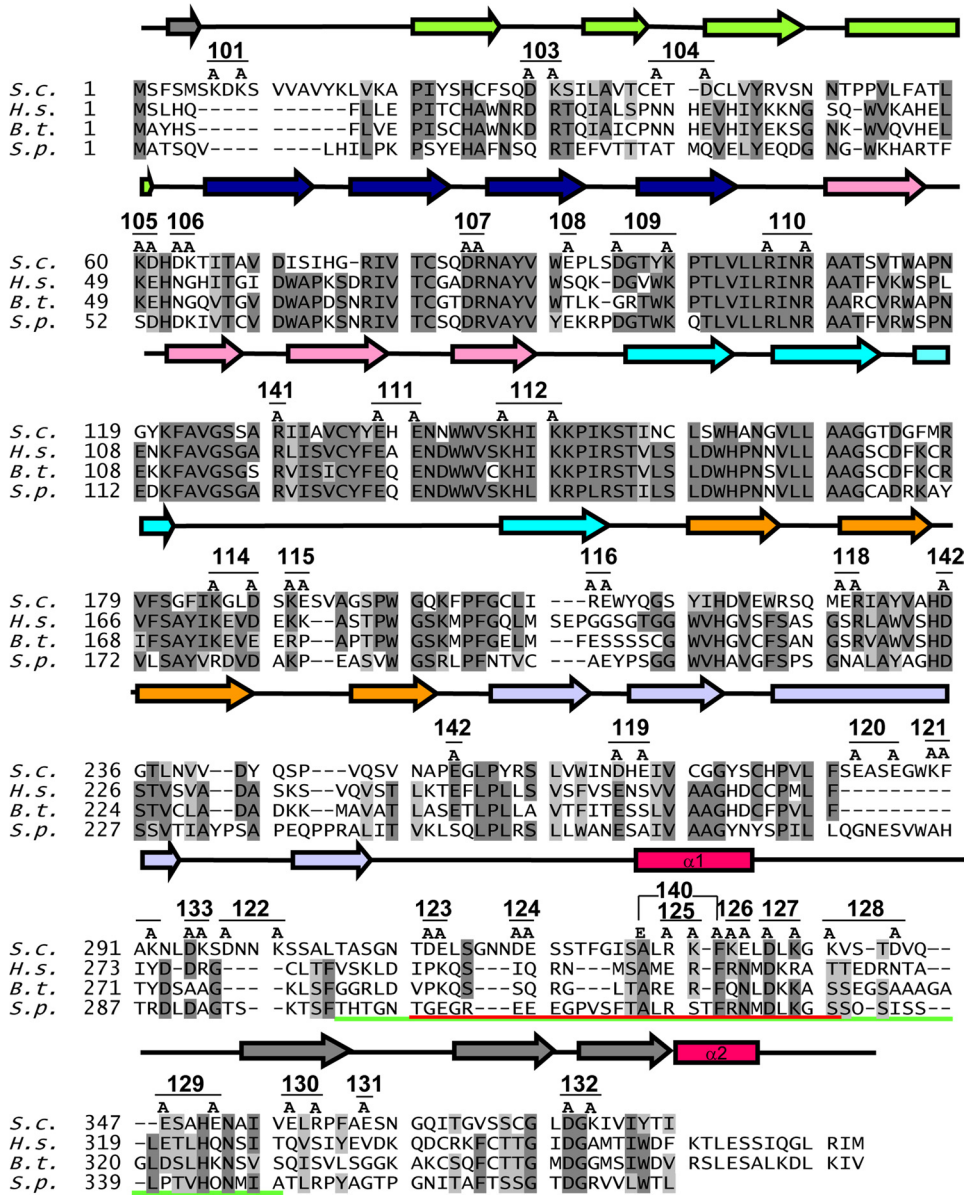

FIGURE 1. **Alignment of p40/ARPC1 primary sequences from *S. cerevisiae* (*S.c.*), *H. sapiens* (*H.s.*), *B. taurus* (*B.t.*), and *S. pombe* (*S.p.*).** Bovine structural elements are designated above the primary sequences. The *arrows* represent β-sheets, and *boxes* represent α-helices. The seven propeller blades of p40/ARPC1 are colored-coded: *green* (blade 1), *blue* (blade 2), *pink* (blade 3), *cyan* (blade 4), *orange* (blade 5), *lavender* (blade 6), and *gray* (blade 7), so that numbering is consistent with Fig. 2. Residues that are identical in all four species are shaded in *dark gray*; similar residues are shaded in *light gray*. Allele numbers and mutations are shown above the *S. cerevisiae* sequence. Sequences internally deleted in *arc40Δ311–340* are marked by a *red line*. Residues included in the arm domain peptide (residues 306–355) are underlined in *green*.

proximal alleles (Table 1, *arc40-139* to *arc40-145*). As discussed in greater detail below, this included combining alleles that make contacts with p19/ARPC4 (encoded by the *ARC19* gene in *S. cerevisiae*) and alleles that comprise a broad exposed surface of p40/ARPC1 that a homology modeling study had predicted binds to the mother filament (17). In addition, we constructed several new alleles, targeting p40/ARPC1 contacts with p15/ARPC5 (encoded by the *ARC15* gene in *S. cerevisiae*) and an exposed α-helix in the structural arm located between propeller blades six and seven of p40/ARPC1 (see below).

We integrated the new *arc40* alleles at the *LEU2* locus of a diploid strain (BGY84) heterozygous for the *arc40* deletion (*arc40Δ/ARC40*). The diploids were sporulated, and tetrads were dissected. Because the *LEU2* and *ARC40* loci segregate independently, we observed for both wild type and pseudo-wild type alleles integrated at the *LEU2* locus the three predicted tetrad growth patterns (two, three, or four viable spores) (Fig. 3*A*; *ARC40*, tetrads 7, 3, and 1, respectively). In contrast, diploid cells with a lethal *arc40* allele integrated at the *LEU2* locus produced only the one predicted pattern of tetrad growth, consisting of two viable spores and two dead spores (Fig. 3*A*; *arc40-139*, *arc40-140*, *arc40-141*, and *arc40-143*). As an independent test of lethality, the same alleles were integrated at the *LEU2* locus of a haploid *arc40Δ* strain carrying a *URA3*-marked *ARC40* plasmid. These strains were plated on medium containing 5-fluoroorotic acid to counterselect against the *URA3*-marked plasmid. This analysis verified that the same alleles fail to complement the loss of wild type *ARC40* (Fig. 3*B*).

To determine whether the lethal *arc40* alleles fell into single or multiple complementation groups, we performed genetic crosses to generate diploid strains carrying pairwise combinations of lethal alleles, covered by the *URA3*-marked *ARC40* plasmid. These strains were tested for growth on 5-fluoroorotic acid. All of the diploid strains failed to grow, demonstrating that none of the lethal alleles complement each other. Thus, all of the lethal alleles fall into a single genetic complementation group (supplemental Fig. S2). One lethal allele (*arc40-143*) was not included in this analysis because of likely defects in folding (see below).

Essential Roles for Intersubunit Contacts—By examining the surface interactions between p40/ARPC1 and p19/ARPC4 in the crystal structure of Arp2/3 complex, we observed that six residues on p40/ARPC1 form a total of eight hydrogen bonds with p19/ARPC4. Four of the six residues are conserved between *Bos taurus* and *S. cerevisiae*, but only one is charged (Arg^{108} in *S. cerevisiae*). This residue forms hydrogen bonds with two residues in p19/ARPC4 (Gln^{28} and Asp^{29} in *B. taurus*) and is changed to alanine in one of our alleles, *arc40-110*. We noted that *arc40-107* is proximal to *arc40-110*, and although it

TABLE 1
Summary of *ARC40* alleles

Allele	Mutation	Growth phenotype	Possible interaction
ARC40	Wild type	NE[a]	
arc40-101	K7A,D8A,K9A	NE	
arc40-103	D30A,K31A	NE	
arc40-104	E39A,D41A	NE	
arc40-105	K60A,D61A	NE	
arc40-106	D63A,K64A	NE	
arc40-107	D83A,R84A	NE	p19/ARPC4
arc40-108	E90A	NE	
arc40-109	D94A,K98A	NE	
arc40-110	R105A,R108A	NE	p19/ARPC4
arc40-111	E137A,E139A	NE	
arc40-112	K146A,K149A	NE	
arc40-114	K185A,D188A	NE	
arc40-115	K190A,E191A	NE	
arc40-116	R209A,E210A	NE	
arc40-118	E227A,R228A	Slow growth at 37 °C	
arc40-119	D266A,E268A	NE	
arc40-120	E283A,E286A	NE	
arc40-121	K289A,K292A	NE	
arc40-122	D298A,K301A	NE	
arc40-123	D312A,E313A	NE	
arc40-124	D319A,E320A	NE	
arc40-125	R330A,K331A	NE	
arc40-126	K333A,E334A	NE	
arc40-127	D336A,K338A	NE	
arc40-128	K340A,D344A	NE	
arc40-129	E347A,E351A	NE	
arc40-130	E356A,R358A	NE	
arc40-131	E362A	NE	
arc40-132	D376A,K378A	NE	
arc40-133	D295A,K296A	NE	
arc40-139	D83A,R84A,R105A,R108A	Lethal	p19/ARPC4
arc40-140	A328E,F332A	Lethal	VCA domain
arc40-141	R129A	Lethal	p15/ARPC5
arc40-142	D235A,E254A	NE	p15/ARPC5
arc40-143	K146A,K149A,K185A,D188A	Lethal	F-actin?
arc40-144	D94A,K98A,R105A,R108A	NE	F-actin?
arc40-145	R105A,R108A,K146A,K149A	NE	F-actin?
arc40Δ311–340	Deletion of 311–340	Lethal	VCA domain

[a] NE, no effect.

does not appear to participate directly in hydrogen bonding in the crystal structure of (inactive) bovine Arp2/3 complex, its proximity to p19/ARPC4 raised the possibility that upon activation it might be involved in contacting p19/ARPC4 (Fig. 3*C*). For this reason, we combined *arc40-107* and *arc40-110* to generate *arc40-139*. This new allele was lethal (Fig. 3, *A* and *B*), suggesting that p40/ARPC1 interactions with p19/ARPC4 are essential for cell viability or, alternatively, that an as-yet-undefined interaction with this surface on p40/ARPC1 is essential.

Upon examining the hydrogen bonding between p40/ARPC1 and p15/ARPC5, we noted that four residues in p40/ARPC1 formed a total of five hydrogen bonds with p15/ARPC5. Three of these p40/ARPC1 residues were conserved between *B. taurus* and *S. cerevisiae*, but none of our existing alleles encompassed these residues. Because two of the residues (Asp^{235} and Glu^{254} in *S. cerevisiae*) were proximal on the surface of p40/ARPC1, whereas the third (Arg^{129} in *S. cerevisiae*) was more distal, we generated two new alleles that mutate these residues, *arc40-141* (R129A) and *arc40-142* (D235A, E254A) (Figs. 1 and 3*D*). *arc40-141* was lethal (Fig. 3, *A* and *B*), whereas *arc40-142* was pseudo-wild type for cell growth and actin organization (not shown). The lethality of the *arc40-141* allele points to the functional importance of this surface on p40/ARPC1, likely because of its physical contacts with the p15/ARPC5 subunit.

The Arc40 Arm Is Essential for Function in Vivo—One of the most interesting features of the p40/ARPC1 subunit is the presence of a largely disordered loop that extends from the well folded β-propeller domain. We refer to this element as the p40/ARPC1 "arm," because it is highly solvent-exposed and would be accessible to potential ligands of p40/ARPC1. The sequence of the arm is relatively divergent but contains a short stretch of more highly conserved residues that can form an α-helix (Fig. 1, residues 328–335 in *S. cerevisiae*). This helix is evident in the packed crystal structure of bovine Arp2/3 complex, where the helix in one complex contacts the Arp3 subunit in an adjacent complex (3). Although it is not yet clear whether this α-helix also exists when the Arp2/3 complex is free in solution, the solvent exposure and sequence conservation of this site suggests that it may promote protein-protein interactions important for Arp2/3 complex function and/or regulation.

Our initial charge-to-alanine collection contained several alleles with mutations in the arm (*arc40-123* to *arc40-128*), but these alleles conferred pseudo-wild type phenotypes. To further investigate the role of this domain, we generated an allele that deleted most of the loop, residues 311–340, replacing it with a five-alanine linker (*arc40Δ311–340*). This allele was lethal, suggesting that it has a crucial role in p40/ARPC1 function (Fig. 3, *A* and *B*). Because mutations of the conserved charged residues in this region were pseudo-wild type (Fig. 1 and Table 1), we considered that conserved hydrophobic residues in the helix might be important for function. Two residues that are absolutely conserved across distant species are Phe^{332} and Ala^{298} (Fig. 1). We generated two new alleles to investigate their roles. First, we changed Phe^{332} to alanine because this Phe residue contacted Arp3 in the crystal structure, but this mutation caused no growth defects (not shown). However, combining the F332A mutation with an A328E produced a lethal allele (*arc40-140*; Fig. 3, *A*, *B*, and *E*). The Ala to Glu substitution was chosen to maintain helical structure while disrupting hydrophobic interactions. The lethality conferred by this allele suggests that this sequence may facilitate an interaction that is critical for Arp2/3 function *in vivo*.

Putative F-actin Binding Site on p40/ARPC1—One previous modeling study hypothesized that a large number of conserved surface residues on p40/ARPC1 contact the mother actin filament (17). Some of these residues were mutated in our *arc40* alleles, but all of them were pseudo-wild type for cell growth and actin organization. We investigated the functional contribution of this surface further by combining four of the alleles in this region (*arc40-109*, *arc40-110*, *arc40-112*, and *arc40-114*; Figs. 1 and 3*F*) in pair-wise combinations and examined their growth phenotypes. One combination allele, *arc40-143* (*arc40-112* and *arc40-114*; Fig. 1), was lethal (Fig. 2, *A* and *B*), whereas the other combinations were pseudo-wild type (not shown). However, the lethality may be due to protein misfolding, because GST-Arc40-143 purified from *E. coli* was unstable compared with wild type GST-Arc40 (not shown), leaving the *in vivo* importance of the putative mother filament binding surface in question.

Effects of Lethal Alleles on Arp2/3 Complex Activity—Next, we investigated how the actin nucleation capabilities of Arp2/3 complex are affected by each lethal *arc40* allele. Accomplishing this required developing a new method for isolating mutant Arp2/3 complexes. Although small quantities of yeast Arp2/3 complex can be isolated from nonlethal yeast strains using a

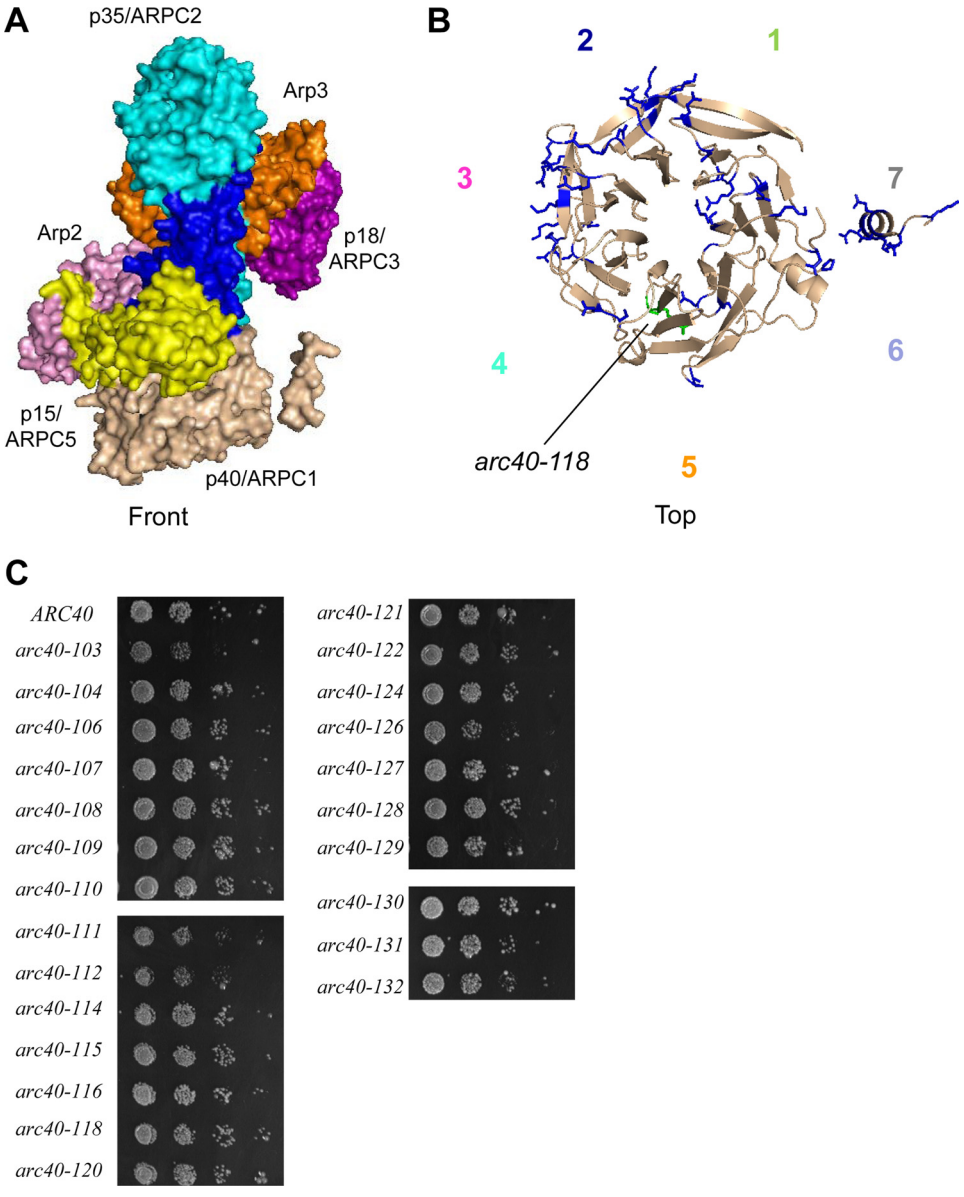

FIGURE 2. **Analysis of initial p40/ARPC1 alanine scan mutations.** *A*, crystal structure of bovine Arp2/3 complex (adapted from Ref. 3), with the seven subunits differently colored: Arp2 (*pink*), Arp3 (*orange*), p40/ARPC1 (*tan*), p35/ARPC2 (*cyan*), p18/ARPC3 (*purple*), p19/ARPC4 (*blue*), and p15/ARPC5 (*yellow*). *B*, top view of p40/ARPC1 showing the positions of residues mutated in the initial alanine scan allele collection modeled on bovine ARPC1. The one temperature-sensitive allele (*arc40-118*; Fig. S1) is *green*; all other alleles were psuedo-wild type for cell growth and actin organization and are colored *blue*. The propeller blades are numbered 1–7 counterclockwise in the top view and color-coded to be consistent with Fig. 1. The side chains of residues mutated in *arc40* alleles are shown. *C*, growth of integrated *arc40* haploid strains at 25 °C. All of the strains were serially diluted and plated for growth on YPD medium at different temperatures (16, 25, 30, 34, and 37 °C); no defects in growth were observed at any temperature (not shown).

cleavable affinity tag integrated at the C terminus of any one of several different subunits (31), this established strategy precludes purification of Arp2/3 complex from lethal mutants. To overcome this obstacle, we developed a new purification strategy, which has four steps: 1) co-expression in a haploid strain of untagged mutant *arc40* and HA-tagged wild type Arc40; this strain also has a TEV-3xHA tag integrated at the C terminus of Arp2; 2) co-isolation of mutant and wild type Arc40-containing Arp2/3 complexes on HA antibody-coated beads; 3) release of mutant Arp2/3 complex by TEV protease digestion; and 4) a final incubation with HA antibody-coated beads to clear any residual wild type Arp2/3 complex. The wild type Arp2/3 complex purified by this method showed actin assembly activity indistinguishably from wild type Arp2/3 complex isolated by our previous method (not shown).

Wild type and lethal mutant Arp2/3 complexes were compared for their abilities to nucleate rabbit muscle actin polymerization in the presence and absence of full-length Las17/WASp (Fig. 4). In the presence of Las17/WASp, *arc40-139* Arp2/3 complex nucleated actin much less efficiently than wild type complex over a range of concentrations (Fig. 4*B*). However, in the absence of Las17/WASp, its base-line nucleation activity was comparable with wild type Arp2/3 complex (Fig. 4*A*). This suggests that *arc40-139* is impaired specifically in WASp-stimulated actin nucleation. In contrast, *arc40-141* Arp2/3 complex nucleated actin assembly with comparable efficiency to wild type Arp2/3 complex in the presence of Las17/WASp, whereas in the absence of Las17/WASp, it exhibited a 2-fold increase in base-line nucleation activity compared with wild type complex over a range of concentrations (Fig. 4, *C* and *D*). Immunoblotting demonstrated that the increased basal nucleation activity of *arc40-141* Arp2/3 complex was not due to contaminating Las17/WASp (not shown). Finally, *arc40-140* Arp2/3 complex showed little if any nucleation activity in the presence or absence of Las17/WASp (Fig. 4, *E* and *F*). Importantly, similar defects were observed for this mutant using yeast actin instead of rabbit muscle actin (supplemental Fig. S3).

Arc40 Arm Binds to the VCA Domain of Las17/WASp—To better understand the mechanistic basis of the *arc40-140* impairments in actin nucleation shown above, we tested whether this mutation affects binding of the VCA domain of Las17/WASp to the Arp2/3 complex. Previous studies have suggested that the p40/ARPC1 subunit of Arp2/3 complex interacts with the VCA domain (15, 16); however, the location of the VCA-binding site on this subunit has remained unknown. We incubated the soluble GST-Arc40 arm with control beads or beads coated with Las17/WASp or its VCA domain. The GST-Arc40 arm showed binding to both con-

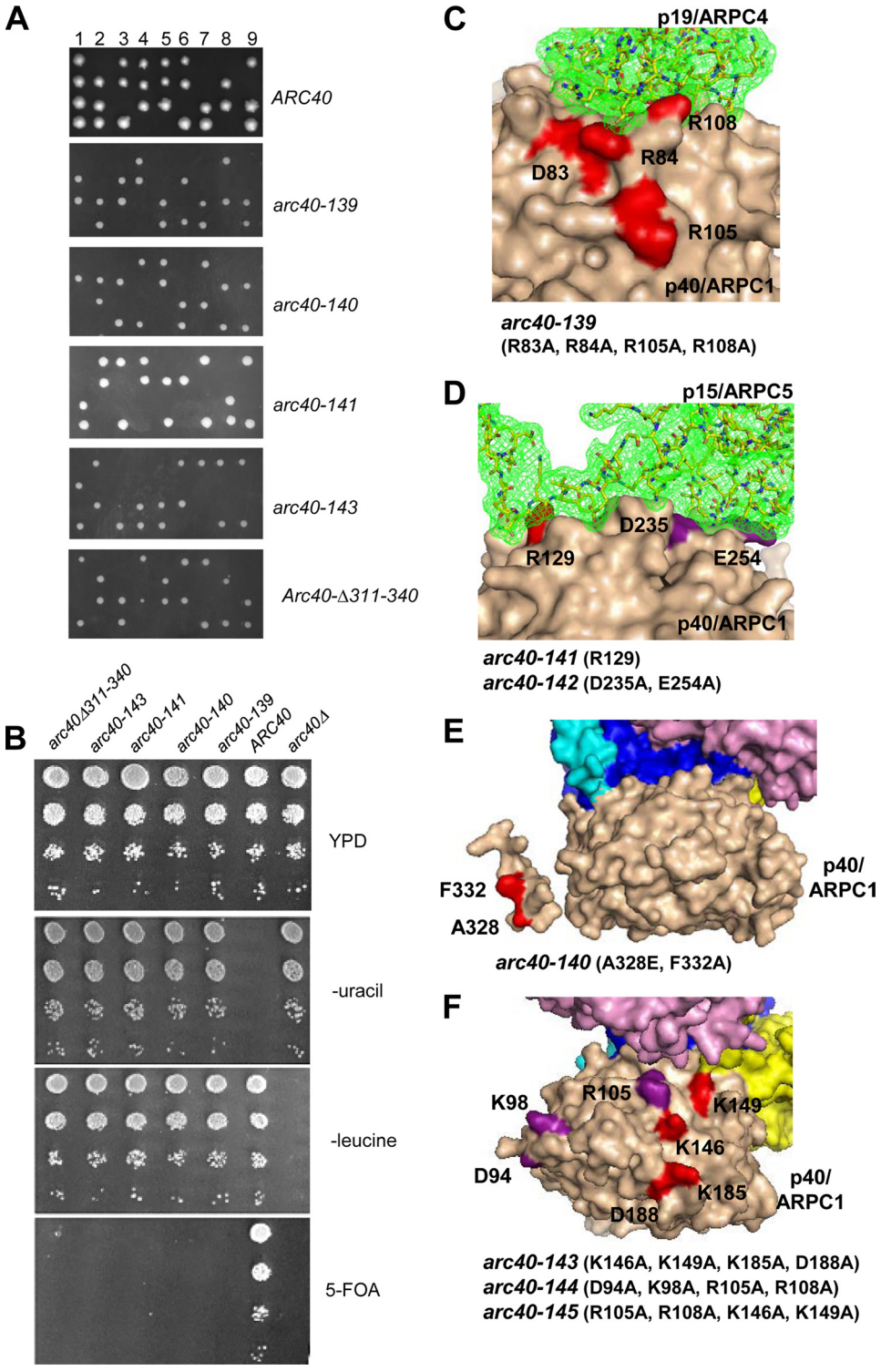

FIGURE 3. **Analysis of lethal *arc40* alleles.** *S. cerevisiae* numbering of residues is used in *C–F*. All of the subunits in the Arp2/3 complex are colored as in Fig. 2*A*. *A*, tetrad analysis of *arc40* alleles integrated at the *LEU2* locus in the heterozygous diploid strain *arc40*Δ::*HIS3/ARC40*. The diploid strains were sporulated, and tetrads were dissected. The specific patterns of growth for all alleles except *ARC40* indicate lethality (see "Results"). *B*, cell growth phenotypes of an *ARC40* strain and *arc40*Δ::*HIS3* strains with integrated *LEU2*-marked copies of *arc40*Δ or specific *arc40* alleles carrying a *URA3* marked *ARC40* plasmid. The cells were grown in YPD medium overnight and then serially diluted, plated on YPD, −uracil, −leucine, or 5-fluoroorotic acid-containing medium, and grown for 3 days at 25 °C. *C*, surface rendered structure of p40/ARPC1 (*tan*) showing its contacts with p19/ARPC4 (stick model with *green mesh*). Residues mutated in lethal *arc40-139* are highlighted in *red* and numbered. *D*, surface rendered structure of p40/ARPC1 showing contacts with p15/ARPC5, with residues in lethal *arc40-141* highlighted in *red*. Residues in nonlethal *arc40-142* are highlighted in *purple*. *E*, surface rendered structure of p40/ARPC1 (*tan*) with residues in lethal *arc40-140* highlighted in *red*. *F*, surface rendered structure of p40/ARPC1 (*tan*) displaying residues that have been predicted to mediate mother filament side binding (17). Mutated residues that when combined yielded a lethal allele (*arc40-143*) are highlighted in *red*. Residues that when combined were pseudo-wild type are highlighted in *purple*.

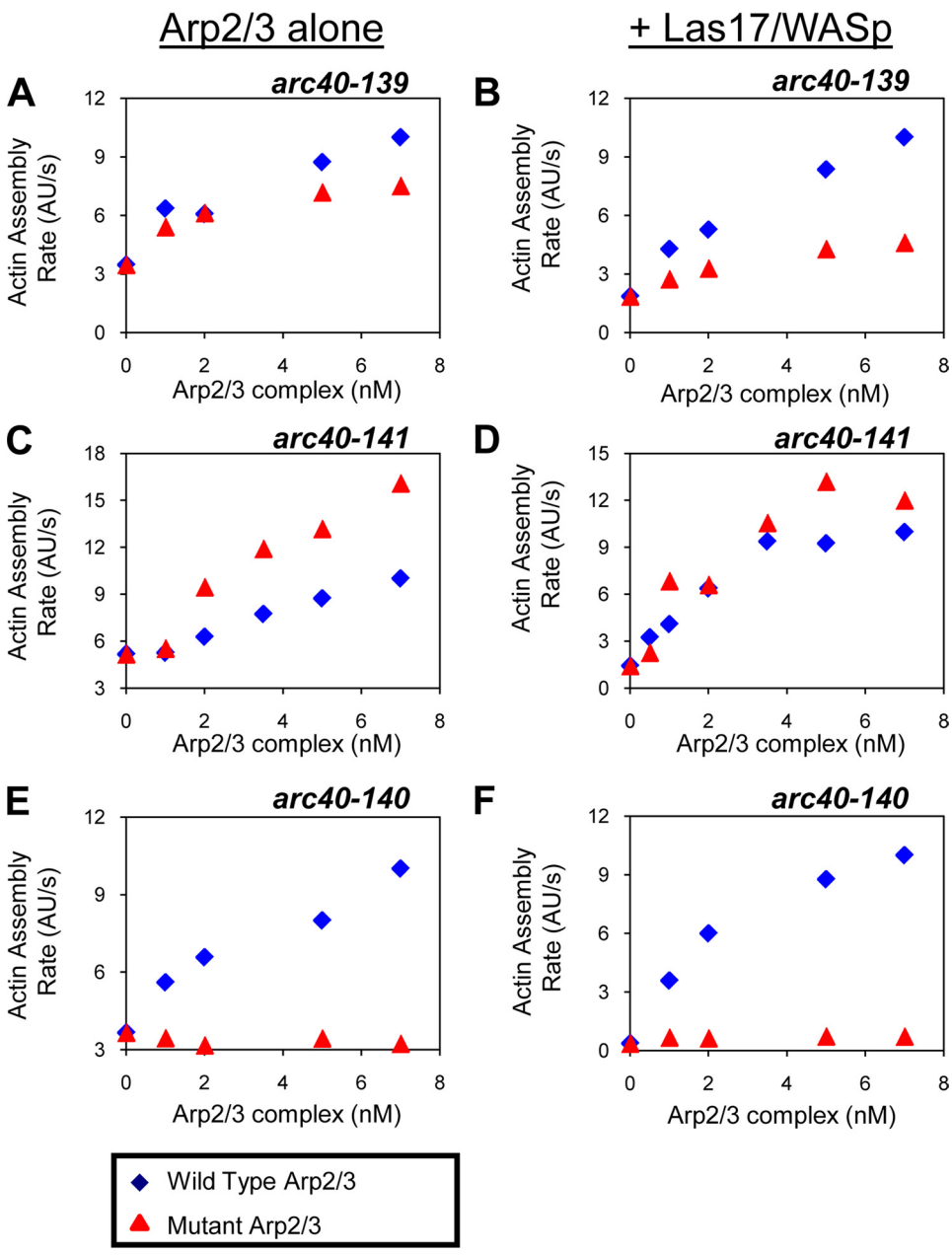

FIGURE 4. **Actin nucleation activities of wild type and *arc40-139, arc40-141,* and *arc40-140* Arp2/3 complexes.** The rates of assembly were determined from the slopes of the curves at their steepest points, which was between 25 and 50% assembly. *A*, *C*, and *E*, actin assembly reactions containing 3 μM monomeric rabbit muscle actin (5% pyrene-labeled) with variable concentrations of wild type (*blue*) or mutant (*red*) Arp2/3 complex. *B*, *D*, and *F*, actin assembly reactions containing 2 μM monomeric rabbit muscle actin (5% pyrene-labeled), Las17/WASp (5 nM for *arc40-139, arc40-141* and 10 nM for *arc40-140*), and variable concentrations of wild type (*blue*) or mutant (*red*) Arp2/3 complex. A higher concentration of monomeric actin was used for the reactions in *A*, *C*, and *E* compared with *B*, *D*, and *F* to more readily detect base-line Arp2/3 complex nucleation activity in the absence of Las17/WASp.

structs but not to control beads, demonstrating that it binds specifically to the VCA domain (Fig. 5*A*). This interaction was verified in reciprocal tests, where soluble Las17/WASp was observed to bind to beads coated with the GST-Arc40 arm but not control beads (Fig. 5*B*). In addition, this interaction was weakened by the *arc40-140* mutation (Fig. 5*B*). Finally, we observed major differences in the abilities of wild type, *arc40Δ311–340* and *arc40-140* Arp2/3 complexes to bind GST-VCA-coated beads (Fig. 5*C*). A deletion of the arm (*arc40Δ311–340*) drastically reduced Arp2/3 complex binding to VCA beads, whereas the double point mutation (*arc40-140*) diminished the interaction to a significant but lesser extent.

Together, these data suggest that one of the critical functions of the Arc40 arm is to interact with the VCA domain of Las17/WASp to promote actin nucleation. Because deletion of the VCA domain of Las17/WASp *in vivo* is not lethal, this further suggests other NPFs genetically redundant with Las17 (*e.g.* Myo3/Myo5 and Pan1) may depend on the same site on the Arc40 arm to activate the Arp2/3 complex.

DISCUSSION

Although a large number of studies have addressed the Arp2/3 complex structure and dissected the effects of many of its cellular NPFs (32), our understanding of the Arp2/3 complex activation mechanism remains incomplete. For instance, it is not yet resolved precisely where on the surface of the Arp2/3 complex NPFs bind or how NPF binding alters the structure and function of some of the subunits in the complex leading to actin assembly. In this study, we used a mutagenesis approach, with coupled genetic-biochemical analyses, to dissect the structure and function of the p40/ARPC1 subunit of Arp2/3 complex. We first identified conserved surface residues on p40/ARPC1 essential for *in vivo* function and then purified the corresponding mutant Arp2/3 complexes and analyzed their defects in WASp-induced actin assembly. In doing so, we identified three essential surfaces on p40/ARPC1 with distinct functional roles in the actin assembly process.

Mutagenesis and in Vivo Analysis—Our initial collection of *arc40* alleles, covering every cluster of conserved charged residues in the primary sequence, failed to identify even a single allele with a strong phenotype. Using the crystal structure of the Arp2/3 complex to model these mutations (Fig. 2*B*), it became evident that these alleles may have lacked stronger phenotypes because of the specific nature of the tertiary fold of p40/ARPC1. Many of the clusters of charged residues mapped to β-sheets that form each propeller blade instead of solvent-exposed surfaces, precluding their involve-

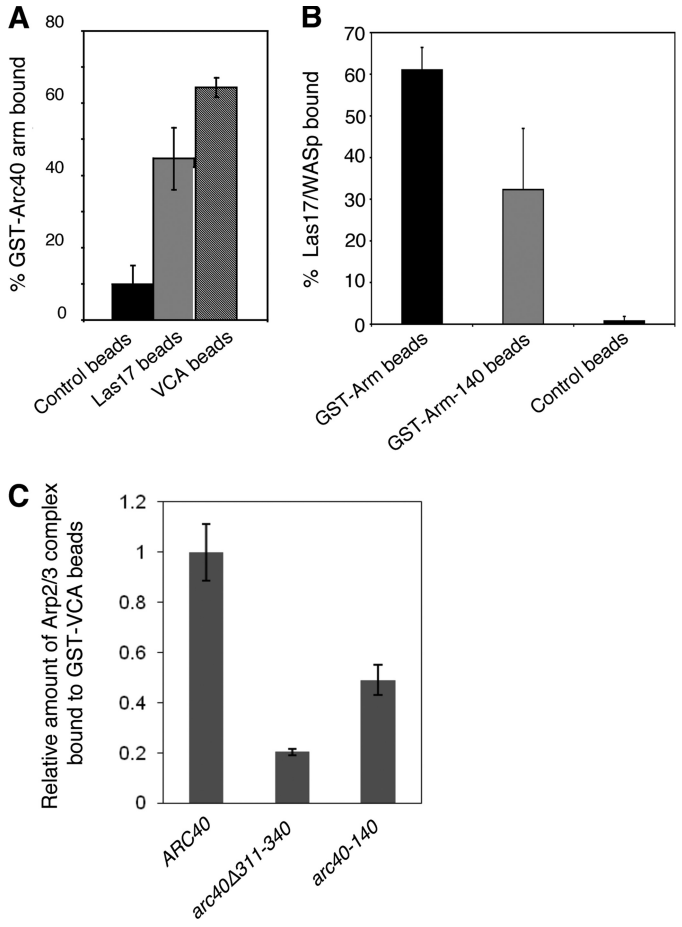

FIGURE 5. **The p40/ARPC1 "arm" domain binds to the VCA domain of Las17/WASp.** *A*, 2 μM soluble Arc40 arm was incubated for 10 min with control beads or beads coated with full-length Las17/WASp or its VCA domain. The beads were pelleted, and the percentage of Arc40 arm bound was determined by analyzing pellets and supernatants on Coomassie-stained gels. *B*, wild type and mutant (*arc40-140*) GST-Arc40 arm peptides were immobilized on glutathione-agarose beads and incubated with 100 nM soluble, full-length Las17/WASp. The beads were pelleted, and the percentage of Las17/WASp bound was determined by analysis of the supernatant fractions by immunoblotting with anti-VCA antibodies. *C*, 75 nM wild type *ARC40*, *arc40Δ311–340*, or *arc40-140* Arp2/3 complex was incubated with GST-VCA coated beads. The beads were pelleted, and the relative amounts of Arp2/3 complex bound were determined by analysis of the pellet fractions by immunoblotting with anti-Arp2 antibodies.

ment in protein-protein interactions. It is interesting to note that these mutations do not appear to disrupt propeller organization and folding because they did not adversely affect cell growth or actin organization. Thus, the p40/ARPC1 β-propeller fold appears to be quite resistant to mutational disruption.

After the crystal structure of bovine Arp2/3 complex became available (3), we modified our mutagenesis strategy (see "Results"), combining specific pairs of first round alleles to generate more new, second round alleles with multiple mutations clustered on proximal surfaces of p40/ARPC1. Using this strategy, we successfully identified three conserved surfaces on p40/ARPC1 that are required for cell viability: 1) sites of contact with p19/ARPC4; 2) sites of contact with p15/ARPC5; and 3) the extended arm domain of p40/ARPC1. Another surface of unknown function on p40/ARPC1, found near its interface with Arp2, was identified as essential for cell viability (*arc40-143*); however, as mentioned, this allele likely caused protein misfolding. Genetic analyses of the remaining three lethal alleles showed that they are each recessive and that they fall into a single complementation group; however, they cause distinct biochemical defects. This implication of these observations is that each of the three functional roles for p40/ARPC1 revealed here (suppression of actin nucleation in the absence of WASp, signaling to other subunits in the complex to promote nucleation in the presence of WASp, and direct binding to the WASp VCA domain) are required for the same physiological function, promoting regulated actin assembly.

p40/ARPC1 Functional Roles in Actin Nucleation—To date, only a limited number of studies have used mutational analyses to dissect Arp2/3 complex structure and function (6, 10, 31, 33). The wild type Arp2/3 complex exists in equilibrium among multiple conformation states, including inactive (open), intermediate, and "primed" (closed) states, with the primed state most closely resembling the conformation of the WASp-bound Arp2/3 complex (6). Mutations in the p35/ARPC2 subunit have been shown to render Arp2/3 complex either less easily activated by WASp (referred to as "nucleation-impaired") or partially active in the absence of WASp (referred to as "unregulated" or leaky), with a corresponding shift in conformational equilibrium toward either the inactive or primed states, respectively (6). A second study showed that mutations in the nucleotide-binding pockets of Arp2 and Arp3 can cause either impaired or enhanced WASp-inducible actin nucleation, with the enhanced activity mutation driving the Arp2/3 complex into a more "closed" conformation (33). A third study revealed that mutations at the barbed end of Arp2 (*e.g. arp2-1* and *arp2-2*) strongly impair actin nucleation in both the presence and the absence of WASp (31). A fourth study dissected the structure and function of the p35/ARPC2 subunit and identified surfaces critical for actin nucleation and endocytosis (10). Here, we have extended these efforts with a dissection of the p40/ARPC1 subunit.

We purified mutant Arp2/3 complexes carrying the lethal alleles identified in our screen (*arc40-139*, *arc40-140*, and *arc40-141*). Analysis of their biochemical activities revealed that *arc40-139* causes the Arp2/3 complex to be nucleation-impaired specifically in response to WASp (Fig. 4, *A* and *B*). This defect is reminiscent of *arc35-6* (6), which suggests that the interaction between p40/ARPC1 and p19/ARPC4 may be important when the complex adopts an activated conformation after WASp binding. In contrast, *arc40-141* caused the Arp2/3 complex to be unregulated in its nucleation activity (Fig. 4, *C* and *D*). These effects are reminiscent of *arc35-5* and *arp2-7* (6, 31), suggesting that the interaction between p40/ARPC1 and p15/ARPC15 may help hold the Arp2/3 complex in an inactive state when NPFs are not present, suppressing nucleation. Because p15/ARPC5 physically interacts with p40/ARPC1 and Arp2, our data suggest that p15/ARPC5 may function as a molecular "latch," holding p40/ARPC1 and perhaps Arp2 in a less active position until WASp triggers conformational rearrangements in the complex that are propagated in part via p19/ARPC4 interactions with p40/ARPC1. Details of this hypothesized mechanism may become clear once a crystal structure of activated Arp2/3 complex becomes available. Finally, *arc40-140* caused the Arp2/3 complex to be nucleation-impaired in

both the presence and the absence of WASp (Fig. 4, *E* and *F*). These effects are reminiscent of *arp2-1 and arp2-2* effects (6, 31) but are more severe. This may explain why *arc40-140* is lethal, whereas *arp2-1* and *arp2-2* are only conditionally lethal (34).

It is interesting to note that in our entire screen, the only lethal mutation we identified in p40/ARPC1 that did not map to a contact interface with another subunit was *arc40-140*. The two residues mutated in this allele (Ala^{328} and Phe^{332}) are found in the extended arm of p40/ARPC1, a segment that is largely disordered in the bovine Arp2/3 complex crystal structure. The location of this arm domain and the absolute conservation of the two residues mutated in *arc40-140* suggest that this site may mediate important functional interactions with other proteins. Our analysis has shown that the arm binds directly to the VCA domain of WASp and that *arc40-140* weakens this interaction (Fig. 5). These observations expand on previous reports showing that VCA interacts with p40/ARPC1 (13–16), defining Ala^{328} and Phe^{332} as residues mediating p40/ARPC1-VCA interactions. In two of the studies mentioned above, conserved hydrophobic residues in the C and A portions of VCA were suggested to mediate contact with p40/ARPC1 (15, 16). Our analysis potentially identifies Ala^{328} and Phe^{332} as the cognate binding site on p40/ARPC1 for one or both of these parts of VCA.

One observation that we have not yet been able to explain is why *arc40-140* impairs actin nucleation of the Arp2/3 complex in the absence of Las17/WASp (Fig. 4). In the crystal structure of the Arp2/3 complex, the helix mutated in this allele packs up against Arp3 of an adjacent complex (3). Because Arp3 is a structural homologue of actin, this may point to a role for this helix of p40/ARPC1 in mediating Arp2/3 complex interactions with actin, which might explain our results. Indeed, one recent high resolution electron microscopy study has suggested that the p40/ARPC1 arm may be important for Arp2/3 complex binding to the mother filament at branch points (9). Technical obstacles prevented us from determining whether *arc40-140* influences binding of Arp2/3 complex to F-actin; further analysis is needed to test this hypothesis.

A Model for p40/ARPC1 Function—Based on our new findings, we propose a model for the role of the p40/ARPC1 subunit in Arp2/3 complex-mediated actin assembly. First, p40/ARPC1 plays an essential role in suppressing actin nucleation by Arp2/3 complex in the absence of WASp. This is achieved through physical contacts between p40/ARPC1 and p15/ARPC5, which maintain the complex in an inactive state. As mentioned above, p15/ARPC5 may serve as a molecular latch, holding p40/ARPC1 and Arp2 in an idling position until WASp (and/or F-actin) triggers conformational rearrangements in the complex leading to nucleation. Second, the extended arm of p40/ARPC1 binds directly to the VCA domain of WASp, which is essential for nucleation. This arm may provide an important anchoring site for WASp and/or help trigger release of the VCA-bound actin monomer to promote nucleation. In addition, the arm of p40/ARPC1 may mediate interactions with F-actin (see above) and thus be multi-functional. Third, we propose that p40/ARPC1 plays a critical role in transmitting WASp activation signals leading to actin nucleation, specifically through contacts with the p19/ARPC4 subunit. It is possible that contacts between p40/ARPC1 and p19/ARPC4 facilitate the propagation of conformational rearrangements in Arp2/3 complex suggested by recent studies (5, 6).

This model suggests that p40/ARPC1 has a number of critical roles in actin nucleation, explaining why this subunit is indispensable *in vivo* (12). In addition to pinpointing the surfaces on p40/ARPC1 that are critical for its cellular and biochemical functions, our data support an emerging view that the specific roles of the individual subunits in Arp2/3 complex are highly integrated and that their interactions with WASp and each other propagate complex structural and functional rearrangements to provide cells with an exquisitely regulated actin nucleation mechanism.

Acknowledgments—We are extremely grateful to D. Sousa and D. Robins for assistance in the early phases of this work. We also thank F. Chaudhry, M. Gandhi, and C. Gould for helpful comments on the manuscript.

REFERENCES

1. Mullins, R. D., Heuser, J. A., and Pollard, T. D. (1998) *Proc. Natl. Acad. Sci. U.S.A.* **95,** 6181–6186
2. Stradal, T. E., Rottner, K., Disanza, A., Confalonieri, S., Innocenti, M., and Scita, G. (2004) *Trends Cell Biol.* **14,** 303–311
3. Robinson, R. C., Turbedsky, K., Kaiser, D. A., Marchand, J. B., Higgs, H. N., Choe, S., and Pollard, T. D. (2001) *Science* **294,** 1679–1684
4. Kelleher, J. F., Atkinson, S. J., and Pollard, T. D. (1995) *J. Cell Biol.* **131,** 385–397
5. Goley, E. D., Rodenbusch, S. E., Martin, A. C., and Welch, M. D. (2004) *Mol. Cell* **16,** 269–279
6. Rodal, A. A., Sokolova, O., Robins, D. B., Daugherty, K. M., Hippenmeyer, S., Riezman, H., Grigorieff, N., and Goode, B. L. (2005) *Nat. Struct. Mol. Biol.* **12,** 26–31
7. Bailly, M., Ichetovkin, I., Grant, W., Zebda, N., Machesky, L. M., Segall, J. E., and Condeelis, J. (2001) *Curr. Biol.* **11,** 620–625
8. Gournier, H., Goley, E. D., Niederstrasser, H., Trinh, T., and Welch, M. D. (2001) *Mol. Cell* **8,** 1041–1052
9. Rouiller, I., Xu, X. P., Amann, K. J., Egile, C., Nickell, S., Nicastro, D., Li, R., Pollard, T. D., Volkmann, N., and Hanein, D. (2008) *J. Cell Biol.* **180,** 887–895
10. Daugherty, K. M., and Goode, B. L. (2008) *J. Biol. Chem.* **283,** 16950–16959
11. Machesky, L. M., and Insall, R. H. (1998) *Curr. Biol.* **8,** 1347–1356
12. Winter, D. C., Choe, E. Y., and Li, R. (1999) *Proc. Natl. Acad. Sci. U.S.A.* **96,** 7288–7293
13. Weaver, A. M., Heuser, J. E., Karginov, A. V., Lee, W. L., Parsons, J. T., and Cooper, J. A. (2002) *Curr. Biol.* **12,** 1270–1278
14. Zalevsky, J., Grigorova, I., and Mullins, R. D. (2001) *J. Biol. Chem.* **276,** 3468–3475
15. Pan, F., Egile, C., Lipkin, T., and Li, R. (2004) *J. Biol. Chem.* **279,** 54629–54636
16. Kelly, A. E., Kranitz, H., Dötsch, V., and Mullins, R. D. (2006) *J. Biol. Chem.* **281,** 10589–10597
17. Beltzner, C. C., and Pollard, T. D. (2004) *J. Mol. Biol.* **336,** 551–565
18. Egile, C., Rouiller, I., Xu, X. P., Volkmann, N., Li, R., and Hanein, D. (2005) *PLoS Biol* **3,** e383
19. Guthrie, C., and Fink, G. (1991) *Methods Enzymol.* **194,** 1–863
20. Cross, F. R. (1997) *Yeast* **13,** 647–653
21. Xu, Y., Moseley, J. B., Sagot, I., Poy, F., Pellman, D., Goode, B. L., and Eck, M. J. (2004) *Cell* **116,** 711–723
22. Longtine, M. S., McKenzie, A., 3rd, Demarini, D. J., Shah, N. G., Wach, A., Brachat, A., Philippsen, P., and Pringle, J. R. (1998) *Yeast* **14,** 953–961
23. Goode, B. L., Wong, J. J., Butty, A. C., Peter, M., McCormack, A. L., Yates, J. R., Drubin, D. G., and Barnes, G. (1999) *J. Cell Biol.* **144,** 83–98

24. Spudich, J. A., and Watt, S. (1971) *J. Biol. Chem.* **246,** 4866–4871
25. Higgs, H. N., and Pollard, T. D. (1999) *J. Biol. Chem.* **274,** 32531–32534
26. Pollard, T. D., and Weeds, A. G. (1984) *FEBS Lett.* **170,** 94–98
27. Rodal, A. A., Manning, A. L., Goode, B. L., and Drubin, D. G. (2003) *Curr. Biol.* **13,** 1000–1008
28. Kozminski, K. G., Chen, A. J., Rodal, A. A., and Drubin, D. G. (2000) *Mol. Biol. Cell* **11,** 339–354
29. Lappalainen, P., Fedorov, E. V., Fedorov, A. A., Almo, S. C., and Drubin, D. G. (1997) *EMBO J.* **16,** 5520–5530
30. Wolven, A. K., Belmont, L. D., Mahoney, N. M., Almo, S. C., and Drubin, D. G. (2000) *J. Cell Biol.* **150,** 895–904
31. D'Agostino, J. L., and Goode, B. L. (2005) *Genetics* **171,** 35–47
32. Pollard, T. D. (2007) *Annu. Rev. Biophys. Biomol. Struct.* **36,** 451–477
33. Martin, A. C., Xu, X. P., Rouiller, I., Kaksonen, M., Sun, Y., Belmont, L., Volkmann, N., Hanein, D., Welch, M., and Drubin, D. G. (2005) *J. Cell Biol.* **168,** 315–328
34. Moreau, V., Madania, A., Martin, R. P., and Winson, B. (1996) *J. Cell Biol.* **134,** 117–132